

# Emergence of Majorana Fermions as quasiparticles in superconductors

Proгна Banerjee

December 18, 2012

Abstract: Over the last few decades, research in the role of topology in quantum condensed matter has gained interest because of the exotic physics involved and the measurement of new quantities that have both theoretical and experimental importance. In topological materials, Majorana fermions, first envisioned by E. Majorana in 1935 to describe neutrinos, often emerge as (non-fundamental) quasiparticles. Consistent with the general principles of relativity and quantum theory Majorana fermions being neutral spin  $1/2$  particles can be thought of their own antiparticles, having identical creation and annihilation operators. Recently experimental evidence of existence of these elusive particles at the interface between a tiny semiconductor wire and a superconducting electrode has been confirmed. Majorana fermions are expected to be resistant to external perturbations as an outcome of inherently obeying non-Abelian anyonic statistics; hence signifying their potential usage in topological fault tolerant quantum computation.

# 1 Motivation behind the search for Majorana Fermions:

## 1.1 Quantum computation, qubits:

The 2012 Nobel Prizes were awarded to David J. Wineland and Serge Haroche for their basic work on understanding the quantum world which may lead to a feasible quantum computer. For over two decades now quantum computer has increasingly become more common in scientific articles, highlighted in different research groups webpage and paved its way into science fiction. But what really is quantum computation and how does that affect the modern society?

Simply put, it is a computing device that embodies the practical application of purely quantum mechanical concepts in storing and relaying information. According to Moores law the circuits on a microprocessor in a computer will be measured on an atomic scale by 2020 or at worst, 2030. The only logical conclusion is to harness the power of the quantum states to achieve a faster, error-free computing device. Presently the basic unit of digital computers is known as bit, that can store information as 0 or 1; only either one of these at a time. In contrast the building block of a quantum computer is dubbed as qubit, here also a maximum of two variables may be stored, but they are not mutually exclusive. It is entirely possible (and expected) for a qubit to take up any value; 0, 1 and anything in between that may be described as a superposition of the aforementioned states.

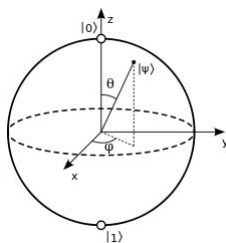


Figure 1: Bloch sphere representation of a qubit. (Wikipedia)

A very important property of the qubit is the entanglement, in which the relayed state depends on the state of the system as observed by the relayer, or more commonly known as the Alice and Bob experiments. This ensures the correct decoding of the data while making quantum cryptography the

most secure system of its kind, the information transmitted and processed depending on many-body systems.

The quantum mechanical nature of these devices make them the best candidates for the next generation of computing, because they can be used to solve complicated problems at a much faster rate than any current computing devices. A quantum computer with  $n$  qubits displays the possibility of being in a superposition of as many as  $2^n$  different states at the same time.

## 1.2 Enter topological quantum computation:

### 1.2.1 Quantum decoherence and Anyons:

An important requirement of any computing device is its ability to remain unaffected by the external environment, so as to preserve the data and to enable error-free transmission of the same. Decoherence or dephasing occurs when the system in question reacts with the surroundings in a thermodynamically irreversible fashion. The ordering or the phase between different components of the system is gradually lost as a result; producing a leakage of information to the surroundings; leading to the appearance of many-body wave-function collapse. Further, decoherence is a major challenge to overcome in the practical implementation of the quantum computer, as any dephasing will severely interfere with the evolution of the quantum states. In order to overcome this difficulty, employing anyons and their non-abelian statistics may be the best solution.

In three-dimensions, or more specifically 3+1 dimensions, all fundamental particles are either fermions or bosons. For particles with a statistics  $\Theta$ , the interchange of any such particles generates a phase of  $e^{i\pi\Theta}$ , whereas the loop of any particle around the other generates a phase of  $e^{2i\pi\Theta}$ . An exchange of two particles is equivalent to one particle executing a half loop around the other, so that a closed loop is equivalent to the exchange squared. The integer values  $\Theta_B = 2j$  and  $\Theta_F = 2j + 1$ , where  $j = 0, 1, 2$ , describe the familiar boson and fermion exchange statistics (abelian) respectively.

However, when these particles are confined to move in 2+1 dimensions, as found in fractional quantum Hall states, the elementary collective excitations of these particles exhibiting fractional charge and statistics are called Anyons. Due to their fractional statistics, upon exchange of two such quasiparticles; the quantum state of a system acquires a phase which is neither 0 nor  $\pi$ , but can be any value. This is because in two dimensions a closed loop executed by

a particle around another particle is topologically distinct from a loop which encloses no particles, unlike the three-dimensional case. This paves the way for topological quantum computation, where the worldlines of anyons cross over in one another to form braids in 3+1 dimensional spacetime. Here, the topology of these quasiparticles plays a huge role in determining their many-body wavefunction. Also environmental decoherence is eliminated from the picture because it is impossible to affect many-particle states.

### 1.2.2 Where do Majorana fermions fit in this picture?

So far, the primary requirements of a futuristic quantum computer has been shown to employ anyons obeying non-abelian statistics, and build logic gates by braiding them to eliminate any external disturbances. Majorana fermions are very good candidates for the job as demonstrated below. Majorana particles, first envisioned by E. Majorana in the 1930s are chargeless, spin-1/2 particles generated by real fields  $\psi$ , (so that  $\psi = \psi^*$ ), that are their own anti-particles. Continuing from Diracs relativistic wave equation with the same nomenclature, Majoranas equation, is simply  $i\gamma^\mu(\delta_\mu - m)\psi = 0$ . Because the  $\gamma^\mu$  matrices are purely imaginary, the matrices  $i\gamma^\mu$  are real, and consequently this equation can govern a real field  $\psi$ .

Recent investigations suggest that exotic quasiparticle excitations in a variety of interesting condensed-matter systems are Majorana fermions.

## 2 Emergence of Majorana fermions in superconductors:

Recent interest in topological quantum computation has seen a surge in investigations of Majorana fermions in condensed matter systems. Superconductors are a possible candidate because at the Fermi level, which correspond to the middle of the superconducting gap, the eigenstates are made of superposition of electrons and holes, making them charge-less. The route to Majorana fermions in superconductors can follow a great variety of pathways. Multiple techniques exist due to the generic requirements of removing degeneracies of a superconductor by breaking spin-rotation and time-reversal symmetries, and then closing and reopening the excitation gap. As the gap goes through zero, Majorana fermions emerge as zero-modes bound to magnetic or electrostatic defects. In a 2008 paper, Liang Fu and Charles Kane showed that

conventional spin-singlet, s-wave superconductivity could be used in combination with the strong spin-orbit coupling of a topological insulator. Out of the many proposed ways of reaching the goal of observation and application of Majorana fermions in superconductors, the device containing a 1-D wire with an s-wave superconductor is described here.

## 2.1 Theoretical model:

If a superconductor (S) is brought into contact with a normal metal (N), the Cooper pairs do not disappear abruptly at the S-N interface but leak into the normal metal. This extends superconducting behaviour into the normal metal and simultaneously weakens the superconductivity near the interface of the S-N structure. Most of the recent studies on the proximity effect have been carried out in sub-micron and nanometer scale S-N structures.

Lutchyn et al. and Oreg et al. recently established that the topological phase in Kitaev's model can be obtained by combining a 1D wire with strong spin-orbit coupling, a conventional s-wave superconductor, and a moderate magnetic field. The Hamiltonian that explains the figure 2 below is given by:

$$H = H_{wire} + H_{\Delta} \quad (1)$$

$$H_{wire} = \int dx \psi^\dagger \left( -\frac{\delta x^2}{2m} - \mu - i\alpha\sigma^y \delta x + h\sigma^z \right) \quad (2)$$

$$H_{\Delta} = \int dx \Delta (\psi \uparrow \psi \downarrow + H.c.) \quad (3)$$

The red and blue curves in Fig. 2(b) illustrate the wires band structure when  $h = 0$ . On application of a moderate external magnetic field, a gap is opened at the crossing between the two spinorbit bands due to Zeeman Effect. Due to spin-orbit coupling, the blue and red parabolas respectively correspond to electronic states whose spin aligns along +y and -y. On connecting the semiconducting nanowire to an ordinary s-wave superconductor, due to the proximity effect, a pairing between electron states of opposite momentum and opposite spins occurs and introduces a gap,  $\Delta$ . Because of competition from spin-orbit coupling the magnetic field only partially polarizes electrons in the remaining lower band as Fig 2 (b) indicates schematically. Turning on  $\Delta$  weakly compared to  $h$  drives the wire into a topological superconducting state that connects smoothly to the weak-pairing phase of

Kitaev's toy model. If the Fermi energy  $\mu$  is inside this gap, the degeneracy is two-fold; combining which with an induced gap creates a topological superconductor. Near the ends of the wire, the electron density is reduced to zero, and  $\mu$  drops below the sub-band energies to become large in amplitude. At the points in space where  $E_Z = (\Delta^2 + \mu^2)^{1/2}$ , Majoranas arise as mid-gap bound states, one at either end of the wire.

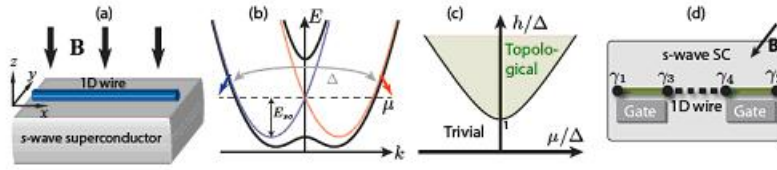


Figure 2: (a) Building blocks for generating Majorana fermions in topological superconducting state, (b) Band structure, (c) Phase diagram, (d) Localized zero-energy Majorana modes. [2]

The influence of the superconducting proximity effect on this band structure can be intuitively understood by focusing on this spinless regime and projecting away the upper unoccupied band, which is legitimate provided  $\Delta \ll h$ . Crucially, because of competition from spin-orbit coupling the magnetic field only partially polarizes electrons in the remaining lower band as Fig. 2 (b) indicates schematically.

## 2.2 Experimental Validation:

In a groundbreaking experiment in 2012, a team from Kavli Institute of Nanoscience, Delft University of Technology and Eindhoven University of Technology[4] have reported the observation of Majorana fermions in hybrid superconductor-semiconductor nanowire devices.

The 1-D nanowire in question is made of InSb, having strong spin-orbit interaction. Mourik et. al. determined a spin-orbit length of about 200 nm and a spin-orbit energy scale of  $50\mu$  eV for this material; with an induced superconducting gap of  $250\mu$  eV. For a ballistic nanowire at zero chemical potential they expect to enter the topological phase for 0.15 T magnetic field. The calculated mean free path in their experiment was near 300 nm, implying a quasi-ballistic regime and these numbers signify that Majorana zero states

are supposed to be measurable below 1 K and at applied magnetic field 0.15 T.

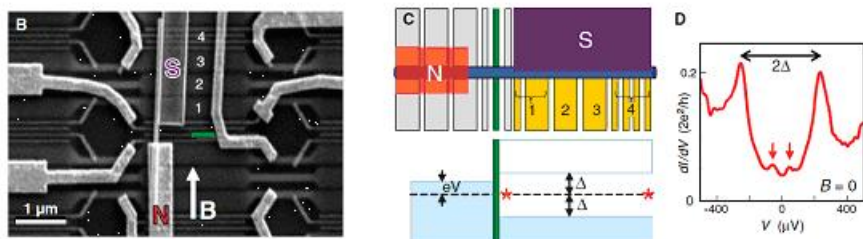


Figure 3: (b) Scanning electron microscope image of the device with normal (N) and superconducting (S) contacts, (c) Top view and energy states, (d) Spectroscopic measurements of DOS. [4]

Experimental methods as taken from Mourik et al's paper [4] are discussed here. They fabricated a pattern of narrow (50 nm) and wider (300 nm) gates on a silicon substrate. InSb nanowires are deposited on these after covering with  $Si_3N_4$  dielectric film. The contacts are made in such a way that the lower one fully covers the bottom part of the nanowire. The bottom gates are crucial for regulation of the device.

It is interesting to ask how electron-doped InSb wires fare as platforms for Majorana fermions. InSb exhibits exceptionally large g factors (50 for bulk crystals), and can be synthesized with high mobility and long mean free paths. Good superconducting proximity effects have also been measured in both systems. One challenge is that while InSb is often lauded as having strong spin-orbit coupling, the energy scale  $E_{so}$  is typically of order 1K. Rashba coupling is gate-tunable to some extent, but it may prove difficult to access the topological phase in a spin-orbit dominated regime where  $h/E_{so} \ll 1$ . Disorder is thus likely to play a nontrivial role in these settings.

By applying a negative voltage to a narrow gate as shown in the figure 3(c) they created a tunnel barrier in the nanowire to perform spectroscopic measurements. This is done so that any applied bias voltage between the normal and the superconductor contacts drop across the tunnel barrier, enabling the measurement of the differential conductance  $dI/dV$ . The other gates tune the density of states in the other regions of the nanowire.

An example of  $dI/dV$  vs  $V$  plot is shown in figure 3(d) at  $B = 0$  and 65 mK, it explores the density of states in the nanowire region below the

superconductor. The value of the induced gap as determined by the authors ( $250 \mu \text{ eV}$ ) is validated in this plot in the observed peaks corresponding to the quasi-particle density of states at that value. The two smaller subgap peaks correspond to the Andreev bound states located symmetrically around zero energy.

### 3 Results: Detection of Majorana fermions:

Despite being chargeless, Majoranas can be detected in electrical measurements. The detection mechanism is a tunneling spectroscopy from a normal conductor into the end of the wire, and looking for a state at zero energy.

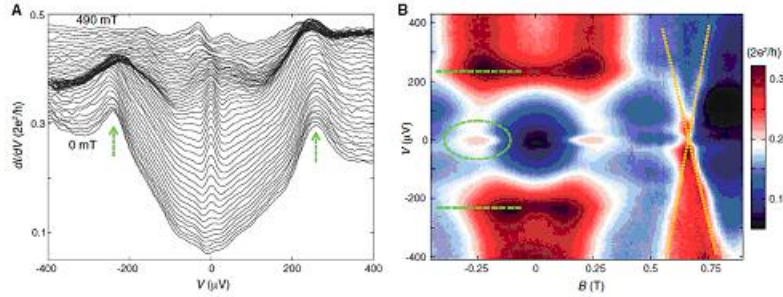


Figure 4: (a)Magnetic field dependent spectroscopy, (b)Color-scale plot, the ZBP is highlighted by a dashed oval; green dashed lines indicate the gap edges. At 600 mT a pair of Andreev bound states are seen. [4]

The Figure 4(a) shows plots of  $dI/dV$ -versus- $V$  traces taken at increasing  $B$  fields in 10-mT steps from 0 (bottom trace) to 490 mT (top trace), offset for clarity. The authors observed the induced gap edges at  $250 \mu \text{ eV}$ . A Zero-bias peak (ZBP) appears at  $B > 150 \text{ mT}$ . The peak has a high amplitude up to  $0.052e^2/h$  to make it distinguishable from the background noise. A pair of Andreev resonances bound within the gap of the bulk NbTiN superconducting electrodes ( $2 \text{ meV}$ ) appear at  $B 600 \text{ mT}$ . The color panel in Fig. 4(b) provides an overview of states and gaps in the plane of energy and  $B$  field from 0.5 to 1 T. The observed symmetry around  $B = 0$  implies the absence of hysteresis.

The zero bias peaks remain unchanged over a wide range of  $B$ . The chances of it being a ZBP from Kondo resonance or reflectionless tunnelling

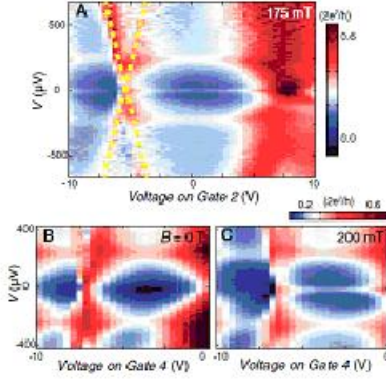


Figure 5: Gate-voltage dependence. (a) A 2D color plot of  $dI/dV$  versus  $V$  and voltage on gate 2 at 175 mT and 60 mK. Andreev bound states cross through zero bias, for example, near 5 V (yellow dotted lines). Split peaks are observed in the range of 7.5 to 10 V. In (b) and (c), the voltage sweeps are shown on gate 4 for 0 and 200 mT with the ZBP absent and present, respectively. Temperature is 50 mK. [4]

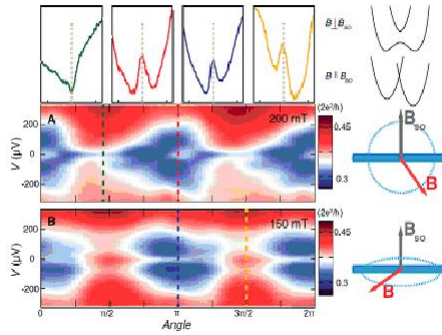


Figure 6: Magnetic-field orientation dependence.  $dI/dV$  versus  $V$  and varying the angle of  $\mathbf{B}$  at fixed magnitude. (a) Rotation of  $\mathbf{B}$  in the plane of  $\mathbf{B}_{SO}$ , (b) Rotation of  $\mathbf{B}$  in the plane perpendicular to  $\mathbf{B}_{SO}$ . The panels on top show linecuts at angles with corresponding colors in (a) and (b). [4]

is ruled out based on the behaviour of the ZBP with changes in magnetic field. In both cases the ZBP shifts its location when  $B$  is changed, which conclusively proves that the one observed in this experiment is indeed the Majorana fermions.

ZBP splits into two peaks symmetric about zero bias at  $B$  400 mT.

Figure 5 shows a color panel with voltage sweeps on gate 2. The peaks in the density of states change with energy when changing gate voltage (highlighted with yellow dotted lines). The ZBP from the previous figure remains stuck to zero bias while changing the gate voltage over a range of several volts. For voltage sweep at gate 4, the ZBP vanishes at  $B = 0$  and emerges at 200 mT. Irrespective of the gate by which the device was controlled, the ZBP displays a stationary behaviour.

To test if spinorbit interaction is crucial for the absence or presence of the ZBP, the  $dI/dV$  versus  $V$  plots are shown in figure 6 while varying the angle for a constant field magnitude. The plane of rotation is approximately equal to the plane of the substrate. As  $B$  is rotated perpendicular to the B-spinorbit, the ZBP center is fixed. However as  $B$  is rotated parallel to the B-spinorbit, the ZBP is lost. The ZBP appears and disappears in accordance with with expectations for the spinorbit direction in the samples.

## 4 Conclusions

The first observation of zero-energy peaks in superconductor-1 D nanowire device is discussed here and the property of the ZBP to rigidly stick to zero energy while changing  $B$  and gate voltages over large ranges indicate that they arise from Majorana fermions, and not from Kondo effect or reflectionless tunnelling. This zerobias peak is absent if any of the necessary ingredients of the Majorana proposals is taken out of the device; that is, the rigid ZBP disappears for zero magnetic field, for a magnetic field parallel to the spinorbit field, or when the superconductivity is eliminated. The ZBP exists over a substantial voltage range for every gate starting from the barrier gate until gate 4, the ZBP can be split in two peaks located symmetrically around zero, and it can never be moved away from zero to finite bias.

## 5 Outlook

The question remains that whether or not the authors in [4] are reporting Majorana fermions or the effects of disorder. Liu et al.[7] ran computer simulations and were able to produce the same Majorana signal by adding disorder to their nanowires.

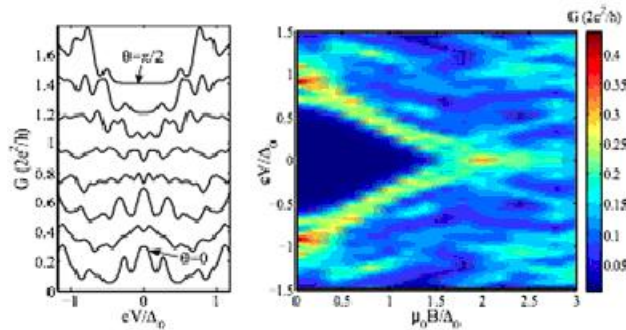


Figure 7: Computer simulations of Majorana signals produced by adding disorder to nanowires [7]

To verify discovery of Majorana fermions, a higher resolution experiment would need to be done at colder temperature to reduce thermal noise.

## 6 Majorana fermions in quantum computing:

The application of Majorana Fermions to store quantum information and hence their application in topological quantum computing is shown here.

The figure 8(a) shows the top view of a 2D topological insulator, contacted at the edge by two superconducting electrodes separated by a magnetic tunnel junction. A pair of Majorana fermions is bound by the superconducting and magnetic gaps. The massless Dirac fermions propagate along a 1D edge state, which is the helical state as seen in quantum spin Hall effect, with the spin pointing in the direction of motion. A Majorana fermion appears as a ZBP at the interface between a s-wave superconductor and a magnetic insulator. Fig 8(a) shows two zero-modes coupled by tunneling in an SIS junction, forming a two-level system (a qubit). The two states  $|1\rangle$  and  $|0\rangle$  of the qubit are distinguished by the presence or absence of an unpaired quasiparticle. For

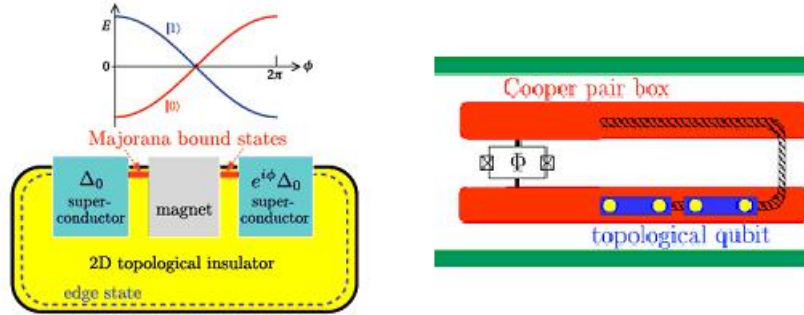


Figure 8: Majorana fermions as qubits in a topological quantum computer, Read out of a topological qubit. [3]

well-separated Majoranas, with an exponentially small tunnel splitting, this is a nonlocal encoding of quantum information: Each zero-mode by itself contains no information on the quasiparticle parity.

To read out a topological qubit one needs to remove the topological protection by coupling the Majorana fermions and then measure the quasiparticle parity. The right hand of figure 8 shows the read out of a topological qubit in a Cooper pair box. It is formed by two pairs of Majorana fermions at the end points of two undepleted segments of a semiconductor nanowire. The charge sensitivity of the Cooper pair box may be tuned by changing the magnetic flux. A pair of Majorana fermions is then moved onto the other island to read the qubit.

## 7 References:

1. F. Wilczek, Nature Physics 5, 614 - 618 (2009).
2. J. Alicea, arXiv:1202.1293 [cond-mat.supr-con].
3. C.W.J. Beenakker, arXiv:1112.1950 [cond-mat.mes-hall].
4. V. Mourik; K. Zuo; S.M. Frolov; S.R. Plissard; E.P.A.M. Bakkers; L.P. Kouwenhoven, Science, arXiv:1204.2792.
5. <http://arxiv.org/ftp/arxiv/papers/0903/0903.2451.pdf>
6. L. Fu and C. L. Kane, Phys. Rev. Lett. 100, 096407 (2008).
7. J. Liu, A.C. Potter, K.T. Law, P.A. Lee arXiv1206.1276v1 6 Jun 2012.